Full Plastic Resistance of Tubes Under Bending and Axial Force: Exact Treatment and Approximations

J. Michael Rotter, Adam J. Sadowski *

Department of Civil & Environmental Engineering, Imperial College London, UK

ABSTRACT

The full plastic resistance under a combination of bending and axial force of tubes of all possible wall thicknesses, from thin cylinders to circular solid sections, does not ever seem to have been thoroughly studied, despite the fact that this is a relatively simple analysis. The first part of this paper presents a formal analysis of the state of full plasticity under longitudinal stresses in a right circular tube of any thickness free of cross-section distortions. The derivation leads to relatively complicated algebraic expressions which are unsuitable for design guides and standards, so the chief purpose of this paper is to devise suitably accurate but simple empirical descriptions that give quite precise values for the state of full plasticity whilst avoiding the complexity of a formal exact analysis. The accuracy of each approximation is demonstrated. The two limiting cases of a thin tube (cylindrical shell) and circular solid section are shown to be simple special cases.

The approximate expressions are particularly useful for the definition of the full plastic condition in tension members subject to small bending actions, but also applicable to all structural members and steel building structures standards, as well as to standards on thin shells where they provide the full plastic reference resistance. These expressions are also useful because they give simple definitions of the orientation of the plastic strain vector, which can assist in the development of analyses of the plastic collapse of arches and axially restrained members under bending.

© 2016 Institution of Structural Engineers. Published by Elsevier Ltd. All rights reserved.

1. Introduction

The full plastic resistance of tubes of all possible wall thicknesses and under all combinations of bending and axial forces does not ever seem to have been thoroughly studied, despite the fact that this is a well-defined problem that requires only a fairly simple analysis. However, the derivation leads to relatively complicated algebraic expressions which are unsuitable for design guides and standards, so the main purpose of this paper is to devise suitably accurate but simple descriptions that give quite precise values for the state of full plasticity whilst avoiding the complexity of a formal exact analysis. Because the condition of full plasticity of the perfect undeformed structure using ideal elastic-plastic material properties is one of the key reference states used in design rules [8,9,16,17], it is important that this state should be accurately defined.

It seems very likely that others may have performed the formal exact analysis for the full plastic condition under both bending and axial force long ago, but the authors have only traced the work of [21] after the review of this paper. Written in French and in a special revue, it was somewhat inaccessible. There consequently seems to be no identifiable basis for the rather varied full plastic interaction expressions used in current standards (e.g. [1–3,8,15]). The focus of this paper is on the development of suitable approximations for application in design guides and standards, as some of the existing approximate rules in standards are shown to be surprisingly inaccurate for such a formally precisely-defined problem.

The formal algebraic analysis of the state of full plasticity in a tube of any thickness is presented here, with the two limiting cases of a thin tube (cylindrical shell) and circular solid section shown as special cases of the full relationship. Because the general equations are too complicated for use in design calculations, two different sets of approximate formulas are presented together with a demonstration of the level of approximation associated with each. Simpler approximations produce greater errors.

These expressions are useful for the definition of the full plastic condition in tubular structural members, with special application for tension members subject to small bending actions, but also applicable to steel building structures standards and standards on thin shells where they provide the full plastic small displacement theory reference resistance. These expressions are also useful because they give simple definitions of the orientation of the plastic strain vector, which can assist in the development of plastic analyses of a particular class of redundant

* Corresponding author.
E-mail address: a.sadowski@imperial.ac.uk (A.J. Sadowski).

structures, including arches and axially restrained members under bending.

It should be recognised that the ultimate resistance of tubular members is affected by many other phenomena: elastic and elastic-plastic stability [7,11,19], ovalisation in long members under bending [4–6, 12,13,18], nonlinearity of the stress-strain relationship in metals other than mild steel [14] and geometric imperfections [10]. All these effects modify the resistance significantly, but the reference resistance against which all these modifications are made is the fully plastic state using an ideal elastic-plastic constitutive law and the undeformed perfect geometry [20]. For this reason, the analysis presented here gives the basic reference case, and it is important that it should be defined with precision.

2. Full plastic cross-section analysis

2.1. Introduction

In line with the terminology used in the Eurocode standard [8], the geometry of a tubular cross-section is here characterised by an external diameter d and a wall thickness t, as shown in Fig. 1. The analysis here treats the material as ideally plastic, with a simple linear yield boundary between the tension and compression zones. The yield boundary is deemed to satisfy the condition of plane sections remaining plane, leading to a straight linear boundary. Because the circular tube is symmetrical about its longitudinal axis, all orientations are identical and only a single orientation needs to be considered for conditions that might be regarded as biaxial bending in a different axis system.

2.2. Reference full plastic resistances under the action of individual stress resultants

The full plastic axial force N_{pl} for a circular tubular cross-section of external diameter d, thickness t and yield stress f_y is simply given by:

$$N_{pl} = \frac{1}{4}\pi\left(d^2 - (d-2t)^2\right)f_y = \pi dt\left(1 - \frac{t}{d}\right)f_y \tag{1}$$

For the limiting case of a circular solid rod ($d/t \to 2$ or $t/d \to 1/2$), this simplifies to:

$$N_{pl} = \frac{\pi}{4}d^2 f_y \tag{2}$$

For the limiting case of a thin tube ($d/t \to \infty$ or $t/d \to 0$), the (t/d) term becomes negligible and Eq. (1) simplifies to:

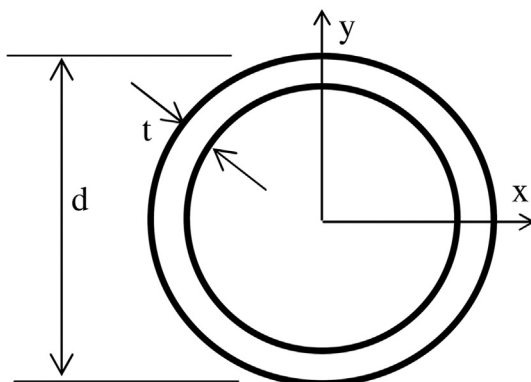$$N_{pl} = \pi dt f_y \tag{3}$$

Fig. 1. Dimensions of the cross-section.

Similarly, the full plastic moment M_{pl} for a finite-thickness tube is given by:

$$M_{pl} = \frac{1}{6}\left(d^3 - (d-2t)^3\right)f_y = \frac{4}{3}d^3\left(\frac{3}{4}\left(\frac{t}{d}\right) - \frac{3}{2}\left(\frac{t}{d}\right)^2 + \left(\frac{t}{d}\right)^3\right)f_y \tag{4}$$

For a solid rod, the limiting case is:

$$M_{pl} = \frac{1}{6}d^3 f_y \tag{5}$$

For a thin tube, the terms $(t/d)^2$ and $(t/d)^3$ become negligible as $t/d \to 0$ and the limiting case is:

$$M_{pl} = d^2 t f_y \tag{6}$$

2.3. Reduced plastic moment in the presence of axial force for the two limiting cases of a solid rod and thin tube

It is appropriate to present briefly the interaction relationship of the plastic moment capacity under the effect of an axial force for the two simpler cases of a solid rod ($d/t \to 2$ or $t/d \to 1/2$) and a thin tube ($d/t \to \infty$ or $t/d \to 0$), as these form the two limiting reference cases against which the more complex relationship of the finite-thickness tube may be verified.

A fully-plastified circular cross-section under a moment M about the centroid and axial force N acting through the centroid undergoes yielding in different proportions in tension and compression depending on the relative magnitudes of these stress resultants (Fig. 2). The Yield Boundary (YB) between tension and compression intersects the exterior surface of the tube at an angle α from the vertical. For the case of pure bending ($N = 0$), $\alpha = \pi/2$ and the YB is coincident with the Centroidal Axis (CA) parallel to the YB.

Due to the doubly-symmetric nature of circular geometries, only the interaction between an axial force in one sense (either tension or compression) ($0 \le \alpha < \pi/2$) and a moment acting in one sense (either sagging or hogging) needs to be considered to obtain the full relationship. For clarity, the image in Fig. 2 shows a section with a larger zone in compression and a smaller zone in tension, but this choice is arbitrary. With this state of plasticity, the yield boundary YB in Fig. 2 moves from lying through the centroid and partitions the lower half of the cross-section into areas under tension A_{T1} and compression A_{C1}. These areas support net forces F_{C1} and F_{T1} acting through the respective centroids of those areas located at distances of y_{C1} and y_{T1} respectively from the CA. The area components and their centroidal distances from the CA may be determined from elementary geometry.

For a solid rod, these are:

$$A_{T1} = \frac{1}{8}d^2(2\alpha - \sin 2\alpha) \quad y_{T1} = \frac{2}{3}d\left(\frac{\sin^3\alpha}{2\alpha - \sin 2\alpha}\right) \tag{7a, b}$$

$$A_{C1} = \frac{1}{8}d^2(\pi - (2\alpha - \sin 2\alpha)) \quad y_{C1} = \frac{2}{3}d\left(\frac{1 - \sin^3\alpha}{\pi - (2\alpha - \sin 2\alpha)}\right) \tag{7c, d}$$

$$A_{C2} = \frac{1}{8}\pi d^2 \quad y_{C2} = \frac{2}{3}\frac{d}{\pi} \tag{7e, f}$$

For a thin tube, these are:

$$A_{T1} = \alpha dt \quad y_{T1} = \frac{1}{2}d\frac{\sin\alpha}{\alpha} \tag{8a, b}$$

$$A_{C1} = \left(\frac{\pi}{2} - \alpha\right)dt \quad y_{C1} = d\left(\frac{1 - \sin\alpha}{\pi - 2\alpha}\right) \tag{8c, d}$$
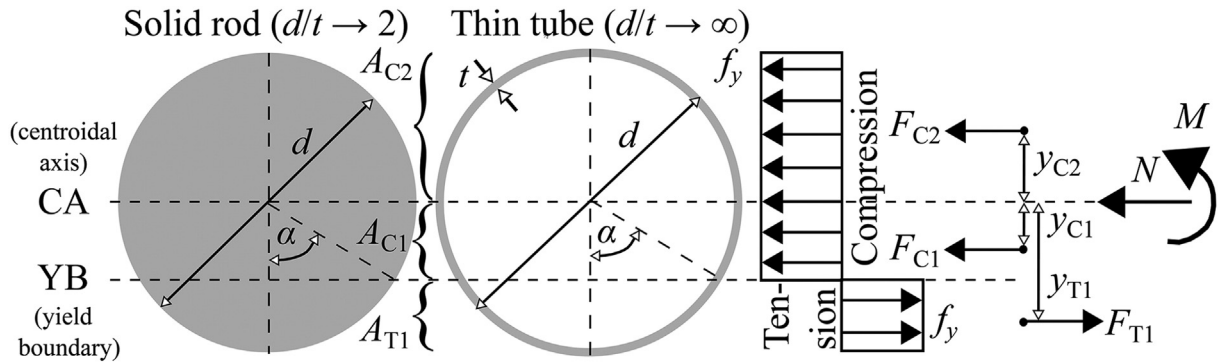
Fig. 2. Circular solid and thin tubular cross-sections at full plasticity under the action of a moment M and compressive force N.

$$A_{C2} = \frac{1}{2}\pi dt \quad y_{C2} = \frac{d}{\pi} \tag{8e, f}$$

The axial force may be determined from equilibrium for either cross-section as:

$$N(\alpha) = F_{C1} + F_{C2} - F_{T1} = \sigma_y(A_{C1} + A_{C2} - A_{T1}) \tag{9}$$

Similarly, taking moments about the CA gives the moment on either cross-section:

$$M(\alpha) = F_{T1}y_{T1} - F_{C1}y_{C1} + F_{C2}y_{C2} = \sigma_y(A_{T1}y_{T1} - A_{C1}y_{C1} + A_{C2}y_{C2}) \tag{10}$$

Substituting and simplifying, the normalised parametric interaction relationships can be written as:

$$n = \frac{N_u}{N_{pl}} = 1 - \frac{(2\alpha - \sin 2\alpha)}{\pi} \quad \text{and} \quad m = \frac{M_u}{M_{pl}} = \sin^3\alpha \quad \text{for a solid rod} \tag{11a, b}$$

$$n = \frac{N_u}{N_{pl}} = 1 - \frac{2\alpha}{\pi} \qquad \text{and} \quad m = \frac{M_u}{M_{pl}} = \sin\alpha \quad \text{for a thin tube} \tag{12a, b}$$

in which the notation N_u and M_u is used to define respectively an ultimate force and moment in the interaction, lying between the fully plastic values of each, N_{pl} and M_{pl}, and the notation n and m is used to identify the dimensionless quantities. The above interaction relationships may also be expressed in closed form as [21]:

$$n = \frac{2}{\pi}\left[m^{1/3}\sqrt{1 - m^{2/3}} + \sin^{-1}\left(\sqrt{1 - m^{2/3}}\right)\right] \quad \text{for a solid rod} \tag{11c}$$

$$n = \frac{2}{\pi}\cos^{-1}(m) \qquad \text{for a thin tube} \tag{12c}$$

Eqs. (11a,b), (11c), (12a), (12b) and (12c) are valid for both tensile and compressive axial forces ($\pi/2 < \alpha \leq \pi$) and for bending moments in either sense (replace M_u by $-M_u$).

2.4. Reduced plastic moment for a finite-thickness tube

2.4.1. Derivation

The derivation of the corresponding relationships for a thick tube is complicated by the fact that the yield boundary YB may be located either fully within the tube material at high axial forces (called 'Region 1' in Fig. 3) or only partially for moderate axial forces (called 'Region 2' in Fig. 4). The limiting boundary between these two regimes is here defined as intersecting the outer surface of the tube at a point that subtends an angle α_B to the vertical. At this boundary the two sets of equations naturally give the same outcome.

$$\alpha_B = \cos^{-1}(1 - 2t/d) \tag{13}$$

2.4.1.1. Region 1) Yield boundary fully inside the tube material ($0 \leq \alpha \leq \alpha_B$).
Under the action of a large compressive or tensile N and accompanying moment M, the yield boundary YB may be located fully inside the tube material. Taking the axial force as compressive (Fig. 3), the cross-section is partitioned into fully-yielded areas A_{C1}, A_{C2} and A_{C3} in compression and A_{T1} tension with corresponding centroidal lever arms and axial forces (Fig. 3).
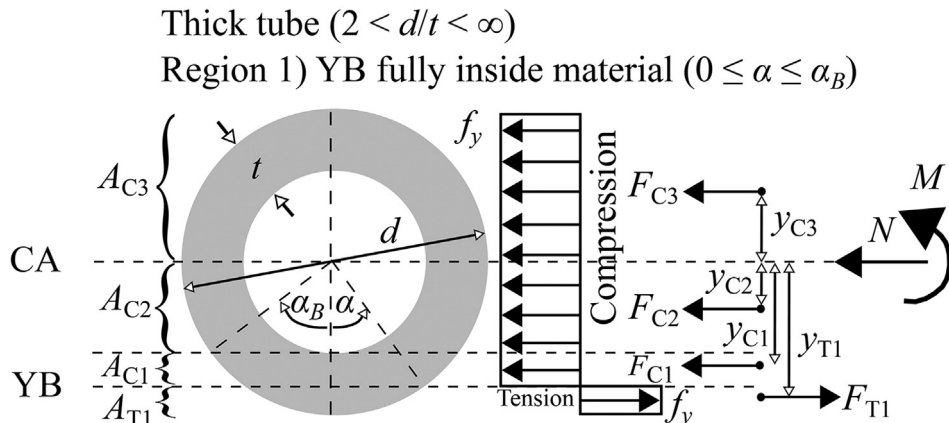

Fig. 3. Thick tubular cross-section at full plasticity under the action of a moment M and compressive force N where the YB lies fully within the material.
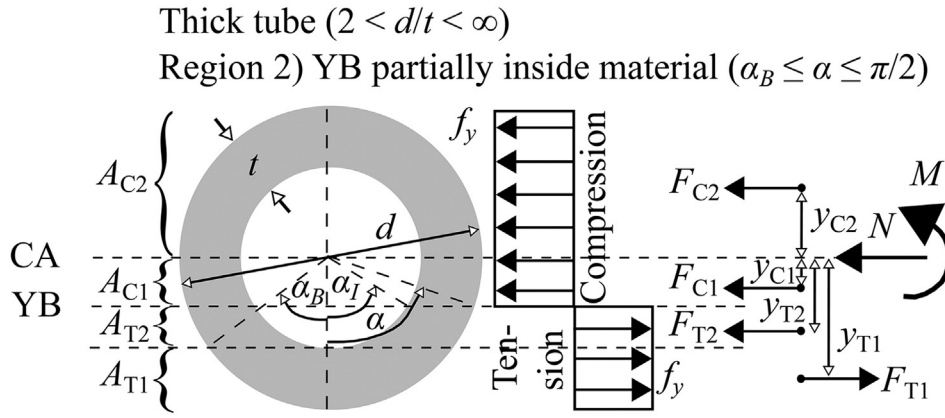
Thick tube ($2 < d/t < \infty$)
Region 2) YB partially inside material ($\alpha_B \leq \alpha \leq \pi/2$)

Fig. 4. Thick tubular cross-section at full plasticity under the action of a moment M and compressive force N where the YB lies partly inside the tube.

In compact form, elementary geometry leads to the following:

$$A_{T1} = \frac{1}{8}d^2(2\alpha - \sin 2\alpha) \quad y_{T1} \frac{1}{12A_{T1}}d^3\sin^3\alpha \tag{14a, b}$$

$$A_{C1} = \frac{1}{8}d^2(2(\alpha_B - \alpha) - (\sin 2\alpha_B - \sin 2\alpha))$$
$$y_{C1} = \frac{1}{12A_{C1}}d^3\left(\sin^3\alpha_B - \sin^3\alpha\right) \tag{14c, d}$$

$$A_{C2} = \frac{1}{8}\left[d^2(\pi - (2\alpha_B - \sin 2\alpha_B)) - \pi(d - 2t)^2\right]$$
$$y_{C2} = \frac{1}{12A_{C2}}\left[d^3\left(1 - \sin^3\alpha_B\right) - (d - 2t)^3\right] \tag{14e, f}$$

$$A_{C3} = \frac{1}{8}\pi\left(d^2 - (d - 2t)^2\right) \quad y_{C3} = \frac{1}{12A_{C3}}\left(d^3 - (d - 2t)^3\right) \tag{14g, h}$$

The net axial force and moment may be obtained from equilibrium:

$$N(\alpha) = F_{C1} + F_{C2} + F_{C3} - F_{T1} = \sigma_y(A_{C1} + A_{C2} + A_{C3} - A_{T1}) \tag{15a}$$

$$M(\alpha) = F_{T1}y_{T1} - F_{C1}y_{C1} - F_{C2}y_{C2} + F_{C3}y_{C3}$$
$$= \sigma_y(A_{T1}y_{T1} - A_{C1}y_{C1} - A_{C2}y_{C2} + A_{C3}y_{C3}) \tag{15b}$$

Substituting and simplifying, the normalised parametric interaction relationships for Region 1 become:

$$n = \frac{N_u}{N_{pl}} = \frac{\pi\left(d^2 - (d - 2t)^2\right) - d^2(2\alpha - \sin 2\alpha)}{\pi\left(d^2 - (d - 2t)^2\right)} \tag{16a}$$

$$m = \frac{M_u}{M_{pl}} = \frac{d^3\sin^3\alpha}{d^3 - (d - 2t)^3} \tag{16b}$$

in which the notation N_u and M_u is again used to define respectively an ultimate force and moment in the interaction between the fully plastic values of each, N_{pl} and M_{pl}.

2.4.1.2. Region 2) Yield boundary partially inside the tube material ($\alpha_B \leq \alpha \leq \pi/2$).
Under the action of a moderate axial force N and bending moment M, the yield boundary YB may be located only partially inside the tube material, partitioning the cross-section into two fully-yielded areas A_{C1} and A_{C2} in compression and A_{T1} and A_{T2} in tension with corresponding centroidal lever arms and axial forces as illustrated in Fig. 4. A further parameter α_I is introduced here to account for the fact that, for a thick tube, the inner and outer tube fibres on the YB occur at different

angular positions relative to the vertical axis.

$$\alpha_I = \cos^{-1}\left(\frac{\cos\alpha}{1 - 2t/d}\right) \tag{17}$$

In compact form, the geometric parameters are as follows:

$$A_{T1} = \frac{1}{8}d^2(2\alpha_B - \sin 2\alpha_B) \quad y_{T1} = \frac{1}{12A_{T1}}d^3\sin^3\alpha_B \tag{18a, b}$$

$$A_{T2} = \frac{1}{8}\left[d^2(2(\alpha - \alpha_B) - (\sin 2\alpha - \sin 2\alpha_B)) - (d - 2t)^2(2\alpha_I - \sin 2\alpha_I)\right] \tag{18c}$$

$$y_{T2} = \frac{1}{12A_{T2}}\left[d^3\left(\sin^3\alpha - \sin^3\alpha_B\right) - (d - 2t)^3\sin^3\alpha_I\right] \tag{18d}$$

$$A_{C1} = \frac{1}{8}\left[d^2(\pi - (2\alpha - \sin 2\alpha)) - (d - 2t)^2(\pi - (2\alpha_I - \sin 2\alpha_I))\right] \tag{18e}$$

$$y_{C1} = \frac{1}{12A_{C1}}\left[d^3\left(1 - \sin^3\alpha\right) - (d - 2t)^3\left(1 - \sin^3\alpha_I\right)\right] \tag{18f}$$

$$A_{C2} = \frac{1}{8}\pi\left(d^2 - (d - 2t)^2\right) \quad y_{C2} = \frac{1}{12A_{C2}}\left(d^3 - (d - 2t)^3\right) \tag{18g, h}$$

The net axial force and moment may be obtained from equilibrium:

$$N(\alpha) = F_{C1} + F_{C2} - F_{T1} - F_{T2} = \sigma_y(A_{C1} + A_{C2} - A_{T1} - A_{T2}) \tag{19a}$$

$$M(\alpha) = F_{T1}y_{T1} + F_{T2}y_{T2} - F_{C1}y_{C1} + F_{C2}y_{C2}$$
$$= \sigma_y(A_{T1}y_{T1} + A_{T2}y_{T2} - A_{C1}y_{C1} + A_{C2}y_{C2}) \tag{19b}$$

Substituting and simplifying, the normalised parametric interaction relationships for Region 2 become:

$$n = \frac{N_u}{N_{pl}} = \frac{\pi\left(d^2 - (d - 2t)^2\right) - d^2(2\alpha - \sin 2\alpha) + (d - 2t)^2(2\alpha_I - \sin 2\alpha_I)}{\pi\left(d^2 - (d - 2t)^2\right)} \tag{20a}$$

$$m = \frac{M_u}{M_{pl}} = \frac{d^3\sin^3\alpha - (d - 2t)^3\sin^3\alpha_I}{d^3 - (d - 2t)^3} \tag{20b}$$

2.4.2. Limiting cases and verifications
As $\alpha \to \alpha_B$ within either region, the two pairs of Eqs. (16a), (16b), (20a) and (20b) naturally tend to the same result, ensuring compatibility, and $\alpha_I \to 0$ within Region 2. Further, in Region 1 Eqs. (16a) and (16b) satisfy $N_u(0) = N_{pl}$, ($n = 1$) and $M_u(0) = 0$, ($m = 0$), whilst in Region 2 Eqs. (20a) and (20b) satisfy $N_u(\pi/2) = 0$, ($n = 0$) and $M_u(\pi/2) = M_{pl}$, ($m = 1$). For the limiting case of a circular solid rod ($t/d \to 1/2$), $\alpha_B \to$

$\cos^{-1}(0) = \pi/2$ and Region 2 ceases to exist, whilst in Region 1 Eqs. (16a) and (16b) reduce to the previous simplified relationship in Eq. (11a,b).

For the limiting case of a thin tube ($t/d \to 0$), $\alpha_B \to \cos^{-1}(1) = 0$, $\alpha_I \to \alpha$ and Region 1 ceases to exist, whilst in Region 2 Eqs. (20a) and (20b) similarly reduce to the previous simplified relationship in Eqs. (12a) and (12b). However, this reduction is not obvious, and must be clarified as follows. Ignoring terms of order $(t/d)^2$, Eq. (20a) may be rewritten:

$$n = \frac{N_u}{N_{pl}} \approx 1 - \frac{1}{4}\frac{d}{t}\left(\frac{2\alpha - \sin 2\alpha}{\pi}\right) + \left(\frac{1}{4}\frac{d}{t} - 1\right)\left(\frac{2\alpha_I - \sin 2\alpha_I}{\pi}\right) \qquad (21)$$

Using Eq. (17), a Taylor series expansion in t/d yields:

$$2\alpha_I - \sin 2\alpha_I = 2\alpha - \sin 2\alpha - 8\sin\alpha\cos\alpha\frac{t}{d} + O\left(\left(\frac{t}{d}\right)^2\right) \qquad (22)$$

Substituting and simplifying:

$$n = \frac{N_u}{N_{pl}} \approx \frac{\pi - 2\alpha}{\pi} + \left(\frac{8\sin\alpha\cos\alpha}{\pi}\right)\frac{t}{d} \to \frac{\pi - 2\alpha}{\pi} \text{ as } \frac{t}{d} \to 0 \qquad (23)$$

which is the result in Eq. (12a).

Similarly, Eq. (20b) may be rewritten by ignoring terms of order $(t/d)^2$ or higher:

$$m = \frac{M_u}{M_{pl}} \approx \frac{1}{6}\frac{d}{t}\sin^3\alpha - \left(\frac{1}{6}\frac{d}{t} - 1\right)\sin^3\alpha_I \qquad (24)$$

Using Eq. (17) and a trigonometric identity, a Taylor series expansion in t/d yields:

$$\sin^3\alpha_I \approx \left(\frac{\sin^2\alpha - 4t/d}{1 - 4t/d}\right)^{\frac{3}{2}} \approx \sin^3\alpha - 6\left(\sin\alpha - \sin^3\alpha\right)\frac{t}{d} + O\left(\left(\frac{t}{d}\right)^2\right) \qquad (25)$$

Substituting and simplifying:

$$m = \frac{M_u}{M_{pl}} \approx \sin\alpha - 6\left(\sin\alpha - \sin^3\alpha\right)\frac{t}{d} \to \sin\alpha \text{ as } \frac{t}{d} \to 0 \qquad (26)$$
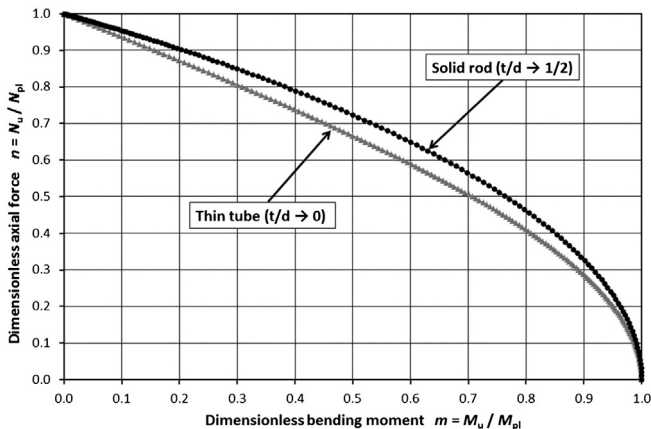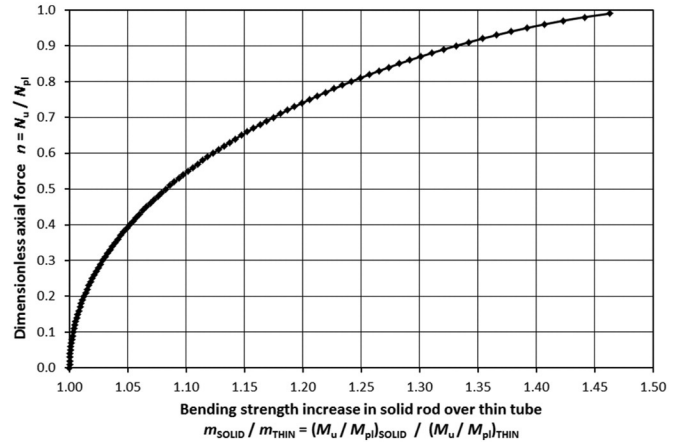
which is the result in Eq. (12b).

Fig. 6. Ratio of the solid to thin shell tube ultimate moments relative to their full plastic moment, each at the same proportion of the full plastic axial capacity.

3. Predictions of the analysis

The exact solution presented above agrees with the bending moment – axial force interaction relationships for the limiting cases of a solid rod ($t/d \to 1/2$) and thin shell ($t/d \to 0$) as shown in Fig. 5. It is evident that there are differences between the relationships for the thin tube and the solid rod, and there is consequently a progressive transition between these two limits for tubes with a finite thickness. Further, since thin shells and slightly thicker tubes are the principal forms of tubular members used in structural design, it is clear that any approximations to be made for design purposes should strive to accurately capture the behaviour close to that of the thin shell, whilst solid sections with small internal holes are probably of lesser practical interest.

The ratio between the bending moment for the circular solid section and the thin shell at a given proportion of their plastic axial forces is shown in Fig. 6. The substantial difference in bending resistance, rising to 50% as the full plastic axial force is approached, shows that any representation of thick tubes that captures the greater resistance at higher axial forces could be very useful in design, especially for tension members.

The full diagram of the plastic limit for tension-compression and sagging-hogging bending is shown in Fig. 7. This marks the bounds of
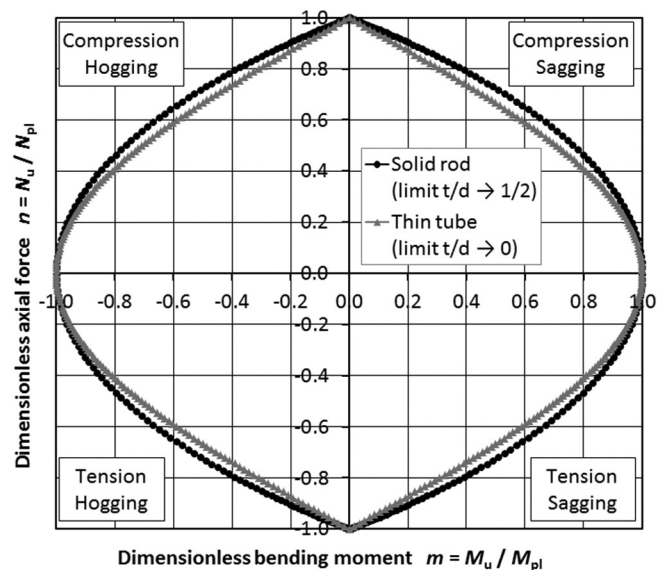

Fig. 5. Limiting interaction diagrams for a thin tube and a circular solid section.

Fig. 7. Complete interaction diagrams for a thin tube and a circular solid section.
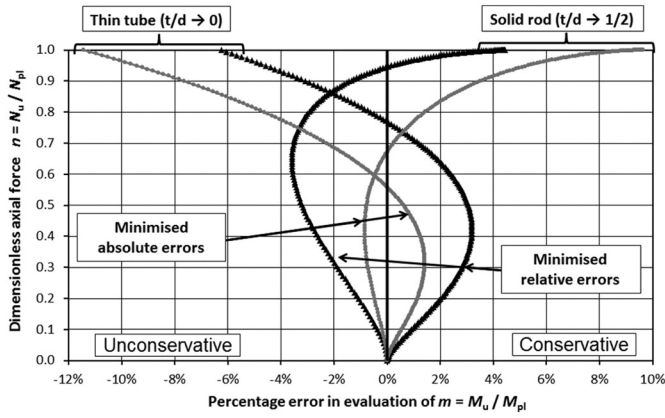
Fig. 8. Errors in estimation of the plastic moment at different axial force using the simple expression in Eq. (27).

all possible states for the cross-section if strain hardening is not included in the analysis, and is useful for those who trace the path of cross-section stress resultant combinations in their finite element calculations, sometimes needed to understand the effects of the normal flow condition.

The interaction for fully plastic cross-section resistances has often been expressed using the simple relationship of the form

$$\frac{M_u}{M_{pl}} = 1 - \left(\frac{N_u}{N_{pl}}\right)^p \quad \text{or} \quad m = 1 - n^p \tag{27}$$

which derives from the exact result for a rectangular cross-section where the power p is exactly 2. The statistical best fits described throughout this study have been undertaken using least squares minimisation of the errors. The best fit simple values of the power p for the thin tube and circular solid rod are found to be 1.75 and 2.13 respectively if the errors are only considered as absolute values, but if the errors are instead expressed as relative $(m_{exact} - m_{fit})/m_{exact}$ to give appropriate weight to errors in smaller values as $N \to N_{pl}$, the values of the power p are found to be 1.673 and 2.25 respectively. These pairs of values both clearly bracket the simple value of 2, but are all much larger than values sometimes used for I-sections under major axis bending (circa 1.30). The percentage errors in the estimation of the exact result using the simple Eq. (27) are shown in Fig. 8. Whilst Eq. (27) is a conveniently simple expression, it is clear that the more practically relevant thin shell tube experiences significantly unconservative errors at high axial forces when represented by this simple formula, especially when the power p is obtained by minimising the absolute errors. By

contrast, the approximation made using relative errors leads to a significant reduction in the unconservatism under high axial forces, which is important for applications involving tension members. The use of relative error minimisation also produces a better balance between unconservative and conservative errors, especially for thin tubes.

One significant advantage of Eq. (27) over the full exact analysis is that it is easy to define the orientation of the normal flow plastic strain vector. In problems concerning complete redundant structures, where a tubular cross-section is treated as an entity, there are situations where the orientation of the plastic strain vector has a significant effect on the resulting plastic deformation and plastic collapse condition. Two such obvious candidates are the plastic collapse of arches, where the interaction of thrust and bending is very significant without stability, and the behaviour of axially restrained members, where axial forces develop as a consequence of changes of geometry under bending. For these and similar situations, the availability of an accurate differentiable expression for the yield surface is of particular value.

For the yield surface of Eq. (27), the plastic strain vector is oriented as

$$\frac{\Delta\kappa}{\Delta\varepsilon} = \left(\frac{N_{pl}}{M_{pl}}\right)\left(\frac{1}{pn^{p-1}}\right) = \left(\frac{N_{pl}}{M_{pl}}\right)\left(\frac{n}{p[1-m]}\right) \tag{28}$$

in which $\Delta\kappa$ is the increment of plastic curvature coincident with the increment of plastic axial strain $\Delta\varepsilon$. By contrast, identifying this orientation using Eqs. (16a), (16b), (20a) and (20b) is a considerable challenge.

Two treatments for tubes of different wall thicknesses are described in what follows. In the first, it is deemed appropriate to retain the simplicity of Eq. (27) and to deduce the variation of the parameter p with the thickness of the tube. This leads to a simpler but less precise definition of the full plastic condition. In the second, a more sophisticated treatment of the form of the interaction is obtained, leading to greater precision at the expense of slightly more complexity.

4. Representation of thicker tubes using Eq. (27) as the interaction expression

Calculations using Eqs. (1)–(26) were performed on a wide range of different tube thicknesses to establish the precise fit value of p in Eq. (27) as the thickness was varied. The thickness of the tube is here represented by the ratio of the thickness to outer diameter (t/d) since this varies between simple limits. It may be noted that manufactured tubes generally lie in the range $0.0 < t/d < 0.135$. A sample of these calculations is shown in Fig. 9. Naturally, these interactions progress
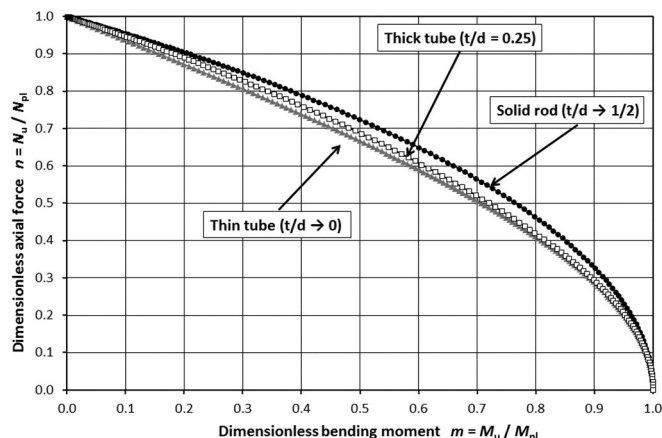

Fig. 9. Exact interaction curves for different tube thicknesses.
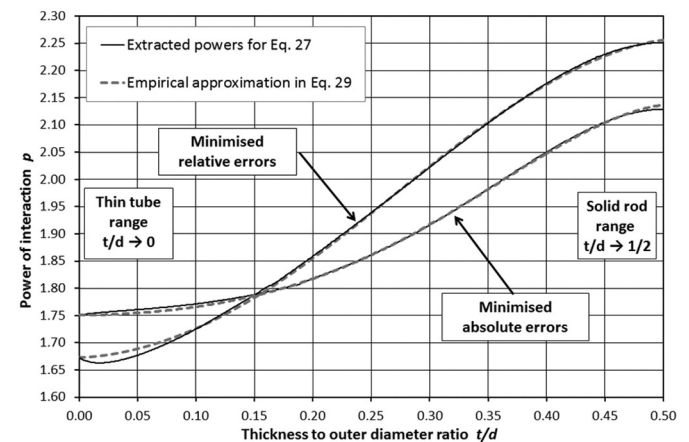

Fig. 10. Variation of the power p in Eq. (27) with tube thickness and the Eqs. (29a) and (29b) approximation.
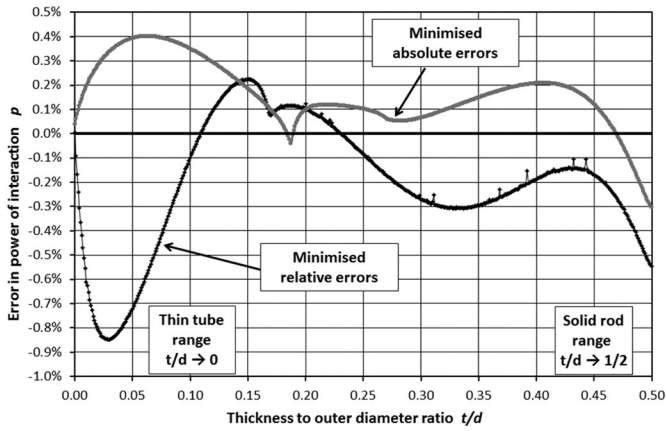
Fig. 11. Errors of Eqs. (29a) and (29b) relative to the extracted power p for Eq. (27) at different tube thicknesses.

Fig. 13. Errors in the estimation of the plastic moment at various axial forces according to Eq. (30).

monotonically from the thin shell to the solid section. The curves are very close together at low axial loads, but significant separation develops at high axial loads, leading to more important errors for tension members subjected to small bending moments.

When these interactions are represented by best fits using Eq. (27), the values of the power p are found as shown in Fig. 10 for both methods of minimising the errors. An initial trial showed that the variations of p with the tube wall thickness could be well represented by a fifth order polynomial, but this has the disadvantage of a lack of transparency. Further work led to a very precise fit using the expressions:

$$p = 1.673 \left\{ \frac{1.61(t/d)^{1.61} + (0.5-t/d)^{1.35}}{1.19(t/d)^{1.61} + (0.5-t/d)^{1.35}} \right\} \text{ for relative errors} \quad (29a)$$

$$p = 1.75 \left\{ \frac{0.787(t/d)^{1.76} + (0.5-t/d)^{1.41}}{0.645(t/d)^{1.76} + (0.5-t/d)^{1.41}} \right\} \text{ for absolute errors} \quad (29b)$$

in which the two limiting values for thin tubes of $p = 1.673$ and 1.75, and for solid rods of $p = 2.25$ ($= 1.673 \times 1.61/1.19$) and 2.13 ($= 1.75 \times 0.787/0.645$), are explicitly identified for the sets of fits assuming relative and absolute errors respectively. The only empiricism lies in the choice of the powers of (t/d) and the functional form. The predictions of this empirical fit are also shown in Fig. 10. The percentage errors in this representation of the variation of the power p relative to the extracted values are shown in Fig. 11, where it is evident that Eqs. (29a) and (29b) provide a very good approximation to the extracted powers when using Eq. (27).
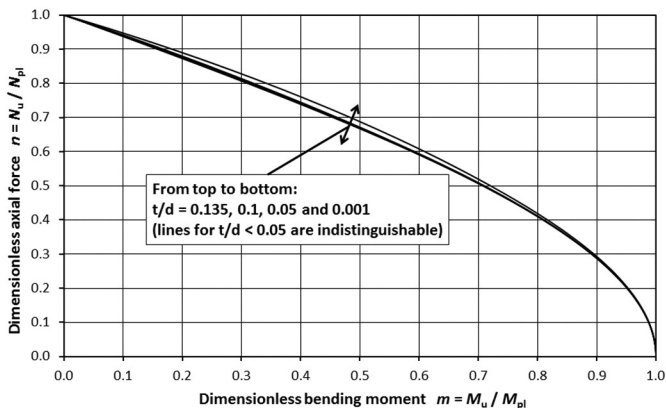
5. Alternative representation of the interaction curve

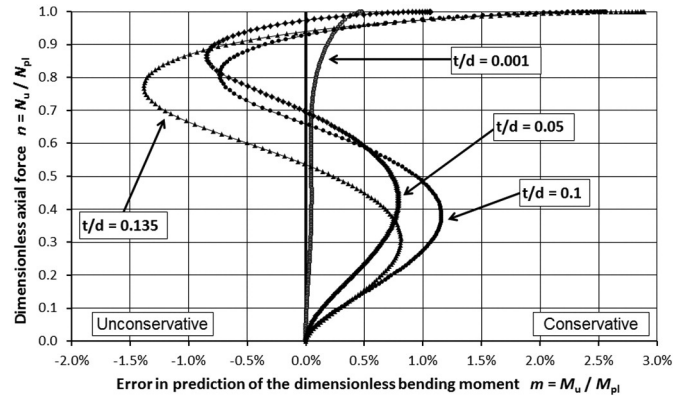The representation of the interaction curve by Eq. (27) produced rather significant errors at high axial forces, as shown in Fig. 8, which are unconservative for thin tubes and could be particularly significant when sections under high tensile forces are being considered for the effect of minor bending. This matter was addressed by considering several slightly more sophisticated relationships for the interaction between bending moment and axial force, resulting in the following outcome.

Since most practical tubes lie somewhere between the ideally thin shell structure ($d/t \to \infty$ or $t/d \to 0$) and thick tubes with a ratio diameter to thickness of around $d/t = 7.5$ or $t/d \approx 0.135$, this range was the focus for an improved interaction rule. In Fig. 10 it is clear that the best fit to the simple expression of Eq. (27) leads to a power p that is relatively stable in this range of t/d, so it is reasonable to suppose that a single better interaction expression might possibly be found for most practical geometries.

Following significant experimentation, it was found that these interactions, using relative error minimisation, could all be very accurately expressed by:

$$m = 1 - n^2 + \left(\frac{n^p - n^2}{b} \right) \quad (30)$$

Fig. 12. Accurate representation by Eq. (30) of the exact interaction.
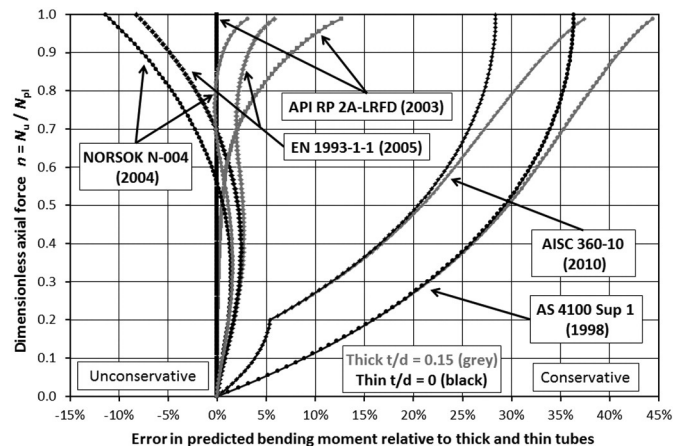

Fig. 14. Errors in estimation of the plastic moment of thin and relatively thick cylinders at different axial force in existing standards for design.
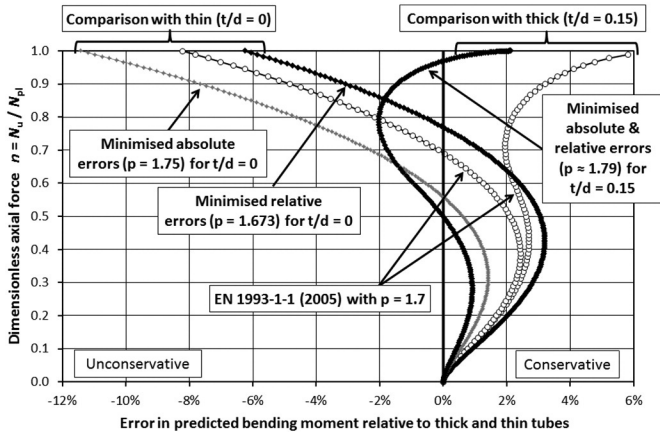
Fig. 15. Errors in estimation by EN 1993-1-1 [8] of the plastic moment of both thick and thin tubes at different axial forces.

in which:

$$p = 3.81 - 22.9(t/d)[1 - 3.36(t/d)] \tag{31}$$

$$b = 0.137 + 2.90(p-2) - 0.38(p-2)^2 \tag{32}$$

The predictions of Eq. (30) are shown in Fig. 12 together with the exact results for values of t/d from zero to 0.135 (or $7.5 < d/t < \infty$). The discrepancies between Eq. (30) and the exact results are shown in Fig. 13. This shows the dramatic reduction in errors compared with either version of the simpler Eq. (27) approximation (Fig. 8). Instead there is an almost exact match for thin tubes (t/d small) and no errors larger than 1.4% for the thickest tubes except at forces above 98% of Npl.

Eqs. (30)–(32) also retain the significant advantage presented by Eq. (27) that it is easy to define the orientation of the normal flow plastic strain vector. This vector is now found as

$$\frac{\Delta\kappa}{\Delta\varepsilon} = \left(\frac{N_{pl}}{M_{pl}}\right)\left\{\frac{b}{n[2(b+1) - pn^{p-2}]}\right\} \tag{33}$$

6. Comparisons with existing standards

Most standards that define the strength of steel structures provide an equation to define the fully plastic condition in circular hollow sections. The provisions of these standards vary, some providing very precise definitions, whilst others less so. The range of tube thicknesses for manufactured tubes is found to be around $7.5 < d/t < 81$ ($0.012 < t/d < 0.135$), though some thicker tubes may be used in some other applications. Thinner tubes are naturally found as cold formed products and as thin shell structures. The comparisons made here focus on these two limits of thickness, and show, at every axial force level, the percentage discrepancy between the defined fully plastic bending moment and the precise value determined from the analysis above. A positive difference indicates a conservative and safe evaluation.

For thin tubular sections and cylindrical shells, a comparison with the limiting case of the thin tube (see Section 2 above) is appropriate. Fig. 14 shows the errors in the expressions used in [1–3,8,15]. The AS 4100 rule uses only an elastic stress limit to define the ultimate plastic resistance, so it is naturally dramatically conservative. The AISC 360-10 rule is not quite so conservative, but still very similar. By contrast, the API RP 2A-LFRD rule follows a trigonometric, rather than power law, interaction between m and n giving the same exact solution for thin tubes ($t/d = 0$) as Eq. (12c). The NORSOK rule is marginally conservative at low axial forces before rising to be rather unconservative at

high axial forces. It prescribes the power law interaction of Eq. (27) with the power $p = 1.75$, so it is identical to the results presented above for minimisation of the absolute errors (Fig. 8). However, relative error minimisation is argued here to be more appropriate, which leads to the lower power $p = 1.673$ and less unconservative predictions at high axial loads (Fig. 8). The expressions in NORSOK, API and AS are intended only for use on tension members, so these ought to give a precise and conservative definition of the bending moment that can accompany a high axial force, rather than providing an accurate definition of the bending resistance at low axial forces.

The effect of the finite thickness of a tube influences the outcome of this comparison, also shown in Fig. 14. Since thicker tubes are marginally stronger than ideally thin tubes, all the predictions of the standards become more conservative, though the difference does not appear to be great on this scale. A clearer message is found by comparing the EN 1993-1-1 [9] provisions for the ideally thin and thickest manufactured tubes, as shown in Fig. 15. Here the thin tube provision is in error in an unconservative sense by just over 8% for high axial loads, whilst for the thick tube this rises to almost 6% in a conservative sense. Also shown for comparison are the errors in the relationships defined by the simple power law interaction in Eq. (27) with Eqs. (29a) and (29b), which illustrate that within the practical range $0 < t/d < 0.15$, the powers p established on the basis of minimised relative errors give less unconservative predictions at high axial loads than those established using absolute errors.

Whilst the conservatism of these estimates of the ideal fully-plastic condition might seem minor, this condition of full plasticity is one of the critical anchor points for all structural assessments [9,16,17] and is thus worthy of an accurate description. The corresponding evaluations for I, H and RHS sections are a standard part of the undergraduate curriculum, so all engineers can perform these calculations accurately and without difficulty. The CHS is worthy of a more accurate treatment with an empirical but precise algebraic representation.

7. Conclusions

This short paper has presented the formal analysis of the state of full plasticity under bending and axial force in a circular tube or cylinder of any thickness. The two limiting cases of a thin tube (cylindrical shell) and a circular solid section have been shown as special cases.

The chief goal of the paper has been to find approximate but simple formulas that can accurately capture the outcome of the general equations, since these are too complicated for use in design calculations. Two different approximate formulas have been presented that are suitable for adoption into design guides and standards. The precision of each has been demonstrated. These expressions also allow easy identification of the orientation of the plastic strain vector on the yield surface, making it easier to formulate plastic collapse analyses of redundant structures in which axial and bending stress resultants strongly interact, such as arches and axially restrained beams.

The accurate representation of the full plastic state in I, H, C and RHS sections involves a simple calculation that is part of the standard training of structural engineers. By contrast, the same analysis for circular tubular sections is not trivial, so it would be appropriate to include accurate expressions in guides and standards for design. The results of this study should be particularly useful for the design of tension members subject to small bending actions.

References

[1] AISC 360-10. Specification for structural steel buildings. Chicago, USA: American Institute for Steel Construction; 2010.
[2] API RP 2A-LFRD. API RP 2A – recommended practice for planning, designing, and constructing fixed offshore platforms—load and resistance factor design. Washington DC, USA: American Petroleum Institute; 2003.
[3] AS 4100-1998. Steel structures. Sydney: Australian Standard, Standards Association of Australia; 1998.
[4] Axelrad EL. On local buckling of thin shells. Int JNonlinear Mech 1985;20(4):249–59.

[5] Brazier LG. On the flexure of thin cylindrical shells and other 'thin' sections. Proc Roy Soc Lond Ser A 1927;116:104–14.

[6] Calladine CR. Theory of shell structures. Cambridge: Cambridge University Press; 1983.

[7] Chen L, Doerich C, Rotter JM. A study of cylindrical shells under global bending in the elastic-plastic range. Steel Constr – Des Res 2008;1(1):59–65.

[8] EN 1993-1-1. Eurocode 3: design of steel structures, part 1-1: general rules and rules for buildings. Brussels: Comité Européen de Normalisation; 2005.

[9] EN 1993-1-6. Eurocode 3: design of steel structures, part 1-6: strength and stability of shell structures. Brussels: Comité Européen de Normalisation; 2007.

[10] Fajuyitan OK, Sadowski AJ, Rotter JM. A study of imperfect cylindrical steel tubes under global bending and varying support conditions. Proc. Eighth International Conference on Advances in Steel Structures; 2015 (Lisbon, Portugal).

[11] Gellin S. The plastic buckling of long cylindrical shells under pure bending. Int J Solids Struct 1980;10:397–407.

[12] Gresnigt AM. Plastic design of buried steel pipelines in settlement areas. Heron 1986;31(4) (113pp).

[13] Karamanos SA. Bending instabilities of elastic tubes. Int J Solids Struct 2002;39(8): 2059–85.

[14] Limam A, Lee L-H, Corona E, Kyriakides S. Inelastic wrinkling and collapse of tubes under combined bending and internal pressure. Int J Mech Sci 2010;52(5):637–47.

[15] NORSOK N-004. Design of steel structures. Lysaker, Norway: Standards Norway; 2004.

[16] Rotter JM. A framework for exploiting different computational assessments in structural design. (Plenary Paper) , Proc. 6th International Conference on Steel and Aluminium Structures, Oxford, 24–27 July; 2007. p. 26–39.

[17] Rotter JM. Advances in understanding shell buckling phenomena and their characterisation for practical design. In: Gizejowski MA, Kowlowski A, Marcinowski J, Ziolko J, editors. Recent progress in steel and composite structures. London: CRC Press, Taylor and Francis; 2016. p. 2–15.

[18] Rotter JM, Sadowski AJ, Chen L. Nonlinear stability of thin elastic cylinders of different length under global bending. Int J Solids Struct 2014;51:2826–39.

[19] Sadowski AJ, Rotter JM. Solid or shell finite elements to model thick cylindrical shells and tubes under global bending. Int J Mech Sci 2013;74:143–53.

[20] Schmidt H, Rotter JM. Rules for the buckling limit state assessment using design by global numerical analysis. In: Rotter JM, Schmidt H, editors. Stability of steel shells: European design recommendations. 5th ed. Brussels: European Convention for Constructional Steelwork; October, 2008. p. 95–145.

[21] Sokol L. Sollicitations ultimes dans une section circulaire pleine (Ultimate resistance in circular sections). Revue Construction Métallique No.2. St Aubin, Paris, France: CTICM; 1988.